Science in China Series E: Technological Sciences

www.scichina.com
tech.scichina.com
www.springerlink.com

Development and distribution of geohazards triggered by the 5.12 Wenchuan Earthquake in China

HUANG RunQiu† & LI WeiLe

State Key Laboratory of Geohazard Prevention and Geoenvironment Protection, Chengdu University of Technology, Chengdu 610059, China

As the Wenchuan Earthquake was of high magnitude and shallow seismic focus, it caused great damage and serious geohazards. By the field investigation and the interpretation of remote-sensing information after the earthquake and by using means of GIS technology, the distribution of geohazards triggered by the earthquake are analyzed and the conclusions are as follows: (1) The earthquake geohazards showed the feature of zonal distribution along the earthquake fault zone and linear distribution along the rivers; (2) the distribution of earthquake geohazards had a marked hanging wall effect, for the development density of geohazards in the hanging wall of earthquake fault zone was obviously higher than that in the foot wall and the width of strong development zone in the hanging wall was about 10 km; (3) the topographical slope was a main factor which controlled the development of earthquake geohazards and a vast majority of hazards were distributed on the slopes of 20° to 50°; (4) the earthquake geohazards had a corresponding relationship with the elevation and micro-landform, for most hazards happened in the river valleys and canyon sections below the elevation of 1500 to 2000 m, particularly in the upper segment of canyon sections (namely, the turning point from the dale to the canyon). Thin ridge, isolated or full-face space mountains were most sensitive to the seismic wave, and had a striking amplifying effect. In these areas, collapses and landslides were most likely to develop; (5) the study also showed that different lithologies determined the types of geohazards, and usually, landslides occurred in soft rocks, while collapses occurred in hard rocks.

5.12 Wenchuan Earthquake, seismogenic geohazard distribution, remote-sensing information, hanging wall effect, GIS analysis

1 Introduction

At 2:28 pm on May 12th, 2008, a devastating earthquake of 8° on Richter scales struck Yingxiu Town of Wenchuan County in Sichuan Province, China (31.0°N and 103.4°E), rupturing the central and front faults in the Longmen Mountain Fault Zone along the the eastern edge of the Tibetan Plateau and forming a coseismic rupture zone of about 300 km in length with 9 m of slip along the boundary between the Longmen Mountain and Sichuan Basin[1]. The damage areas covered more than 130000 km^2, including 39 counties (cities) in Sichuan Province and 12 counties in Gansu and Shanxi provinces along the rupture zone. The Wenchuan Earthquake had high magnitude and strong destructive force with releasing masses of energy and affected vast areas[2], and moreover triggered a large amount of geohazards, especially catastrophic landslides and collapses in the middle and high mountain areas with vulnerable geological environment along the western edge of the Sichuan Basin (Figures 1 and 2). Their huge scale, tremendous numbers, wide coverage, variations in and complexity of types and severe destruction shocked the world. According to statistic data available, the number of collapses and

Received November 13, 2008; accepted February 19, 2009
doi: 10.1007/s11431-009-0117-1
†Corresponding author (email: hrq@cdut.edu.cn)
Supported by the Key Basic Research Program of the Ministry of Science and Technology of China (Grant No. 2008CB425800)

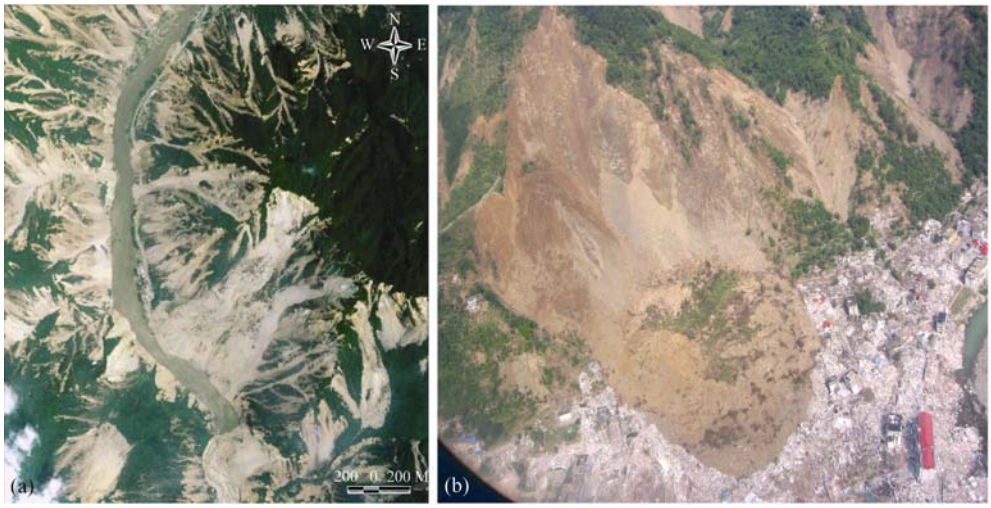

Figure 1 Aerial photos showing the landslides along a section of Mingjiang River (a) and Wangjiayan landslide in Beichuan county town (b).

Figure 2 Photos showing the regional distribution of landslides (a) and Donghekou landslide in Qingchuan County (b).

landslides was about 20000, but the estimated number is over 50000. These geohazards not only caused a large number of casualties and serious economic losses, aggravating the destruction of earthquake, but also put the threats to the post-earthquake rescue, temporary resettlement, and post-reconstruction and rehabilitation in the earthquake-hit areas.

After the earthquake, the authors engaged in the post-earthquake work including the emergency investigation of geohazards, hazard analysis, remote-sensing interpretation of hazard distribution, and geoenvironment assessment for resettlement sites for the locals affected by the earthquake. On the basis of these work, the authors chose the 16 seriously damaged counties along the seismogenic rupture zone as the case study areas (Figure 3) and adopted GIS technology to conduct an investigation of the distribution of geohazards triggered by this huge earthquake as well as the development factors of the geohazards, including the distance from the seismogenic faults, the location relative to the seismic faults, the topographic slopes, and lithologic characters.

2 Post-earthquake field investigation and data acquirement

After the main shock of the Wenchuan Earthquake, the Ministry of Land and Resources of China immediately organized the scientists to conduct the earthquake engineering and geological reconnaissance to provide scientific decision-making information and emergency countermeasures for the postseismic emergency and transitional resettlement sites and reconstruction. The authors were charged with investigation and research on the seismogenic geohazards in the 16 severely damaged counties, of which 10 were extremely damaged and 6 were seriously damaged (Figure 3). This paper presents

one of these investigation achievements.

For investigation, two approaches to get the information and the data on the seismogenic geohazards were: field investigation and remote-sensing image interpretation.

For the areas where the towns and villages were located, and where the investigators could reach, the field investigation was carried out since the potential coseismic and postseicmic geohazards would put the local people's lives and property under the catastrophic risk again. With this approach the information at 4431 seismogenic geohazard spots in the 16 severely damaged counties, including Wenchuan, Beichuan and Qingchuan was obtained. The field at investigation into each geohazard site included mapping, identifing the characteristics of the geohazards and preliminarily assessing the hazard induced potential risk to the locals, buildings and temporary shelters. It is worth to mention that the timely site investigation results were truly effective to make the locals keep from potential dangers and damages.

As a matter of fact, in such an earthquake-hit area, there were numerous collapses and landslides distributed in uninhabited regions, posing indirect threat to human habitat environment. As such geohazards were of large number and wide coverage, it was impossible to do site investigation in such a post-earthquake emergency case. Various remote-sensing data availabe after the earthquake were employed. The main remote-sensing data sources adopted were (1) the image data of Japanese satellite ALOS (10 m resolution), (2) the aerial remote-sensing information obtained by Air Command and China Aero Geophysical Survey and Remote Sensing Center for Land and Resources after earthquake, and (3) other data sources. As ALOS data have wide coverage for a single shot, high quality and resolution ratio, satisfying the requirements for macro-interpretation of geohazards, it was served as the main data source of interpretation, and under the circumstance of cloud cover, the aerial remote-sensing data were employed as a complement.

In the 432 false color composite images of ALOS, the post-earthquake hazards show high brightness, and the image features are clear and easy to recognize so that the computation techniques can be used to deal with the information from ALOS automatically. For calculation of the number of geohazards, the method of human-computer interaction was adopted for the interpretation, and 6877 geohazards were obtained by remote-sensing image interpretation.

Therefore there were 11308 seismogenic geohazard sites in the 16 severely damaged counties, 4431 by field investigation and 6877 by remote-sensing image interpretation.

3 Distribution characteristics of seismogenic geohazards

3.1 Linear distribution along the seismogenic fault

By the site investigation, the number of newly increased seismogenic geohazards in the Wenchuan earthquake-hit areas, which posed a direct threat to human habitat environment reached as many as 9000, mainly distributed in 39 serious disaster counties in Sichuan Province[3]. There were more than 500 newly increased seismogenic hazards in three counties of Wenchuan, Beichuan and Qingchuan, and more than 970 developed in Qingchuan County, the highest among the 39 counties. There were 8 counties each having 300－500 newly seismogenic hazards, i.e., Maoxian, Dujiangyan, Pengzhou, Congzhou, Mianzhu, Wangcang, Jiangyou and Lizhou district of Guangyuan City. There were 17 counties each having 100－300 newly seismogenic hazards (Figure 3)[3]. It can be seen that the counties having a large number of the newly increased geohazards presented a zonal distribution spatially along the Longmen Mountain Fault Zone.

Further, on ArcGIS platform, with the digital elevation model of 1:50000 scale as geographical basic map, the total of 11308 new seismogenic geohazard sites including 4431 by field investigation and 6877 by remote-sensing interpretation were integrated to obtain the spatial distribution of the geohazards in the studied areas (Figure 4). Figure 4 demonstrates that the seismogenic geohazards have a marked feature of zonal distribution.

The results of GIS buffer analysis of geohazard sites within the range of 30 km from the coseismic faults are shown in Table 1. Generally, the farther the distance from the coseismic faults, the less the hazard distribution density. The geohazards developed mainly within 10 km around the coseismic faults, about 2/3 hazards were distributed in these area, and the geohazard density was also the highest, ~1/km^2 on average, and decreased rapidly out of 15 km from the coseismic faults, where the density lowers to 1/6 of that within the areas 5 km from the coseismic faulds, and 1/3 of the density in the areas within 5－10 km. This indicates that the geohazards triggered by the earthquake along the coseismic faults are confined within the zonal area of 15－20 km from

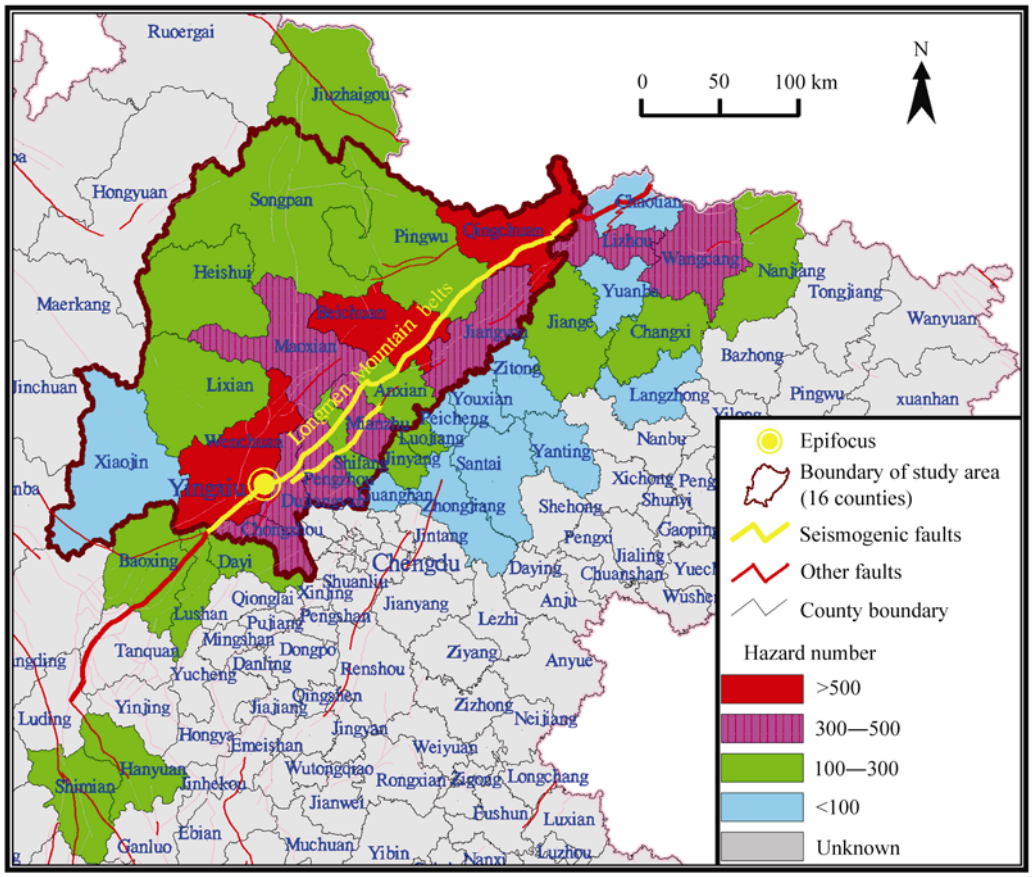

Figure 3 Distribution of geohazards induced by Wenchuan Earthquake[3].

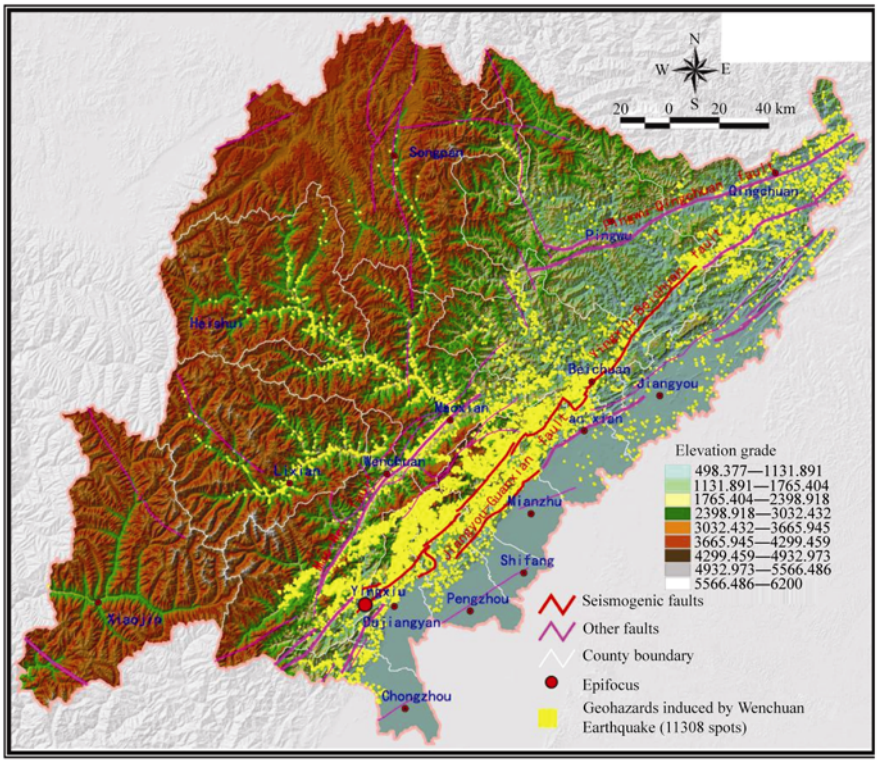

Figure 4 Regional distribution of geohazards in studied area.

Table 1 Relationship between distribution of geohazards and distance from coseismic fault

Distance from seismogenic fault (km)	Area (km^2)	Number of geohazards	Geohazards density (n/km^2)
<5	2918.98	3929	1.35
5—10	2438.06	2224	0.91
10—15	2436.57	1098	0.45
15—20	2552.22	849	0.33
20—25	2556.75	563	0.22
25—30	2492.63	523	0.21

both sides of the faults, in which the area within 10 km from the faults is the most sensitive.

3.2 Hanging wall and foot wall effect

Further study showed that the spatial distribution of the seismogenic geohazards along the faults demonstrated a marked hanging wall and foot wall effect, i.e., the density of geohazards developed in the hanging wall of the faults was much higher than that at the foot wall. The same effect was found in the study of the thrust fault seismogeneration[4—10], e.g., the peak acceleration at the hanging wall surface was greater than that at the foot wall surface under the circumstance of thrust fault seismogeneration, and the damage in the hanging wall was more serious than that in the foot wall. During the Wenchuan Earthquake, it was also found that the houses in the hanging wall of fault were completely collapsed while those at the foot wall remained intact in Beichuan County. The investigation showed that this kind of effect was much more significant during the coseimic geohazard development.

Firstly, the geohazard distribution along the Dujiangyan-Wenchuan section of No. 213 National Highway was investigated, then the statistic analyses of the linear density of geohazard development along the section were conducted, and the damage degrees caused by geohazards to the highway by the ratio of the length of section occupied by waste-mass to the total length of the calculated section were estimated. The results are shown in Figure 5. The 120 km long Dujiangyan-Wenchuan section is across the coseismic Yingxiu-Beichuan fault. In the hanging wall of the fault, the linear density of geohazards was the highest, 11.6/km, and the road damage ratio was 62% in the area of 10—20 km away from the fault. Although the density was quite small in the area of 0—10 km away from the fault, the scales of individual geohazards were larger and the damage ratio was 58% almost the same as that of 10—20 km. The density of geohazards in the section of 0—30 km in the hanging wall was ~6.8/km on average. However, the linear density of coseismic geohazard development in the footw all was within the range of 0.5—0.8/km, being 1/10 of that in the hanging wall. Obviously, the haning wall effect and foot wall effect of the Wenchuan Earthquake were rather striking in the geohazard development.

The areal distribution of seismogenic geohazards also demonstrated a marked hanging wall and foot wall effect. Figure 6 shows the interpretation results of the coseismic geohazards by using the post-earthquake ALOS satellite image of Beichuan, Anxian and Mianzhu counties. The density of seismogenic geohazards in the hanging wall of the Yingxiu-Beichuan Fault was obviously higher than that in the foot wall. The area within 10 km away from the fault in the hanging wall was a strong development zone of the geohazards, in which the areal density reached $3.5/km^2$. The area within 10—20 km was a weak development zone, in which the areal density was $1.5/km^2$. In the foot wall of the fault, no strong development zone existed and only a weak development zone could be found, which, as the hanging wall of the Longmen Mountain front fault, probably was the response to activities of the Longmen Mountain front rupture.

3.3 Linear distribution along rivers

Another marked feature of geohazards triggered by the Wenchuan Earthquake in regional distribution was that they presented linear distribution along rivers, which was clearly demonstrated in Figure 4. The field investigation also indicated that a vast majority of seismogenic geohazards occurred along the two sides of the Minjiang River and along the deep-incised river valleys perpendicular to the NE-SW Longmen Mountain, including the Shiting River, the Mianyuan River and the Qianjiang River as well as their tributaries. These rivers, together with the coseismic structures along the NE-SW Longmen Mountain, control the regional distribution of the geohazards. The coseismic structures control the outline pattern of seismogenic geohazards, while the rivers specifically control their location.

Figure 7 shows the comparison of ETM images of

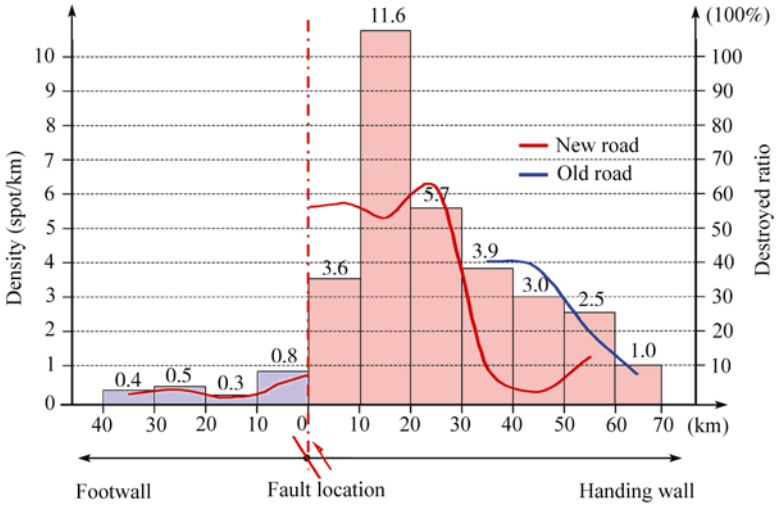

Figure 5 Difference of geohazards development in the hanging wall and Foot wall along the Dujiangyan-Wenchuan section of No. 213 National Highway.

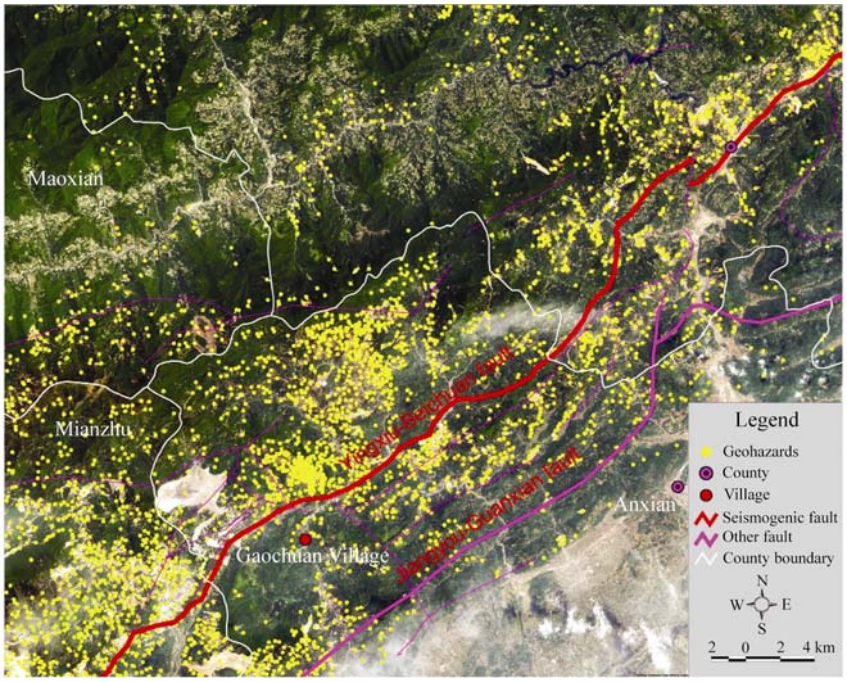

Figure 6 Remote sensing interpretation of geohazards distribution in Beichuan-Anxiang-Mianzhu counties (by ALOS satellite image,10 m resolution).

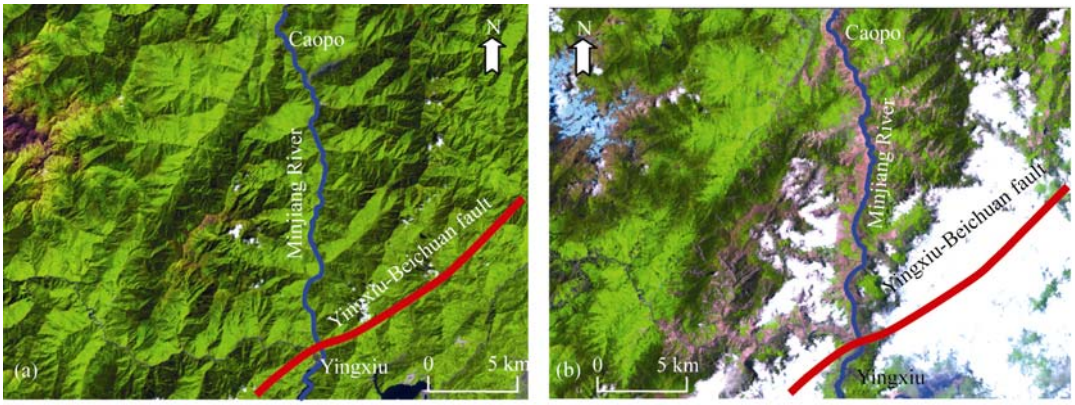

Figure 7 Comparison of ETM images before (a) and after (b) the earthquake (15 m resolution).

Yingxiu-Caopo segment (about 30 km) of the Minjaing River before and after the earthquake. After the earthquake, many collapses and landslides developed along the two sides of the Minjiang River, which are clearly shown in purple colour in the ETM image (Figure 7(a)). This would make the human being astounding at the strength of the Nature.

3.4 Asymmetrical development of geohazards away from the epicenter along coseismic faults

Seismic mechanism study[11,12] shows that the rupturing process of the Wenchuan Earthquake started from Yingxiu Town, spreading to the northeast and southwest by way of bilateral asymmetry. The rupturing to the northeast was obviously stronger than that to the southwest, the former lasted as long as 90 s, and the later only ~60 s. The rupture length to the northeast was much bigger than that to the southwest. Figure 3 shows the difference in the distribution of geohazards along the seismogenic faults: Distribution and density of the geohazards to the northeast from the epicenter are far larger and higher than those to the southwest, which is considered as the response to the seismic rupturing process.

3.5 Seismogenic faults controlling distribution of large (giant) landslides and collapses

The earthquake triggered a large number of large (giant) landslides and collapses, such as Tangjiashan landslide, Wangjiayan landslide and Luanshiyao collapse in Beichuan County, Donghekou landslide, Shibangou landslide, and Woqian landslide in Qingchuan County, Wenjiagou landslide in Qingping Town of Mianzhu City, and Daguangbao landslide in Anxian County. Daguangbao landslide in Anxian County might be the largest landslide both in China and in the world. Table 2 and Figure 8 are the calculation results of the distance between large (giant) landslides and the seismogenic faults. Among the calculated 105 large (giant) landslides, there were 80 landslides which were located less than 5 km away from the seismogenic faults, accounting for 76.19% of the total. The giant landslides including Daguangbao landslide, Tangjiashan landslide, Wangjiayan landslide, Wenjiagou landslide are distributed within this range. There were 98 landslides which were located less than 10 km from the seismogenic fault, 93.33% of the total, and only 7 landslides were located in the areas out of 10 km away from the seismogenic faults. As the distance away from the seismogenic faults increased, the scale of the seismogenic landslides and collapses became smaller. It is suggested that the distribution of large (giant) landslides and collapses is controlled by the seismogenic faults and the seismic wave is the fatal factor triggering large (giant) landslides and collapses on the slope bodies.

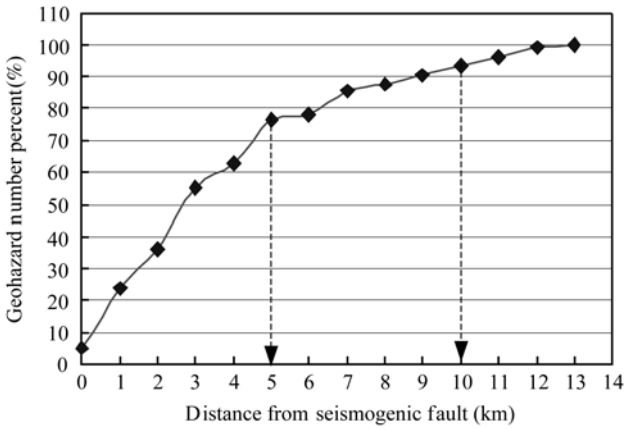

Figure 8 Correlation curve of large geohazards distribution and seismogenic faults.

Table 2 Relationship between distribution of large geohazards and seismogenic faults

Distance from seismogenic fault (km)	Number of geohazards	Percentage of Geohazard numbers (%)
<1	25	23.81
1—2	13	12.38
2—3	20	19.05
3—4	8	7.62
4—5	14	13.33
5—6	2	1.90
6—7	8	7.62
7—8	2	1.90
8—9	3	2.86
9—10	3	2.86
10—11	3	2.86
11—12	3	2.86
12—13	1	0.95

4 Other main factors on seismogenic geohazard distribution

4.1 Elevation

On GIS platform, we conducted a spatial statistic analysis for the distribution elevation of the geohazards, and the results are listed in Table 3 and shown in Figure 9. The seismogenic geohazards were mainly distributed within the range from 650 to 2000 m in elevation. The areas of this range only cover 27% of the totally studied area, but 74.8% of the seismogenic geohazards were distributed in this area, in which the density within the range at the elevation from 1000 to 1500 m was the highest, reaching to 0.63/km^2. The development of the geohazards within the range of more than 2500 m is sparse, and the density of which is only 0.05/km^2.

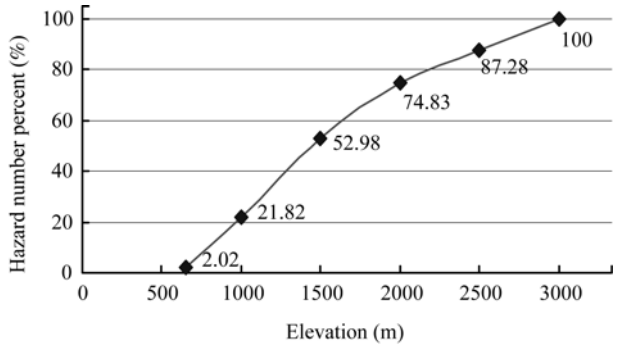

Figure 9 Correlation curve of geohazards distribution and elevation.

Through field investigation, it is found that the development of the seismogenic geohazards is co-controlled by the shape of the river valleys and the elevation. As shown in Figure 10, the area of the river valleys generally took a shape, above the elevation of 1500 m the slope of river valleys is generally gentle, and with elevation lower than 1500 m, the topographic slope turns quite steep, the upper part became the ideal place of unloading of rock mass, while the lower part often constitutes the depositing areas of waste mass resulting from collapses and

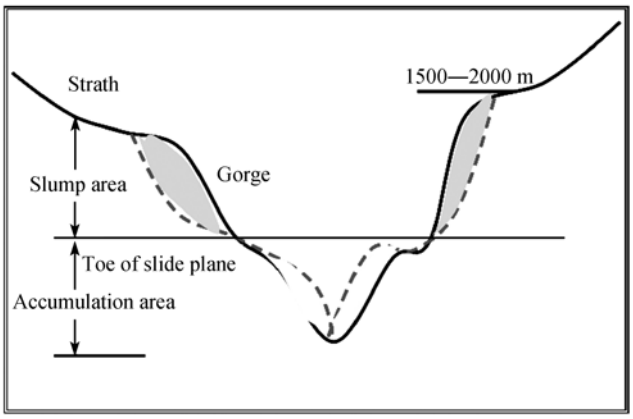

Figure 10 Sketch map of landslide deformation in the transition region from dale to canyon.

landslides. Therefore, the seismic response is the most prominent and the seismogenic geohazards are the most developed in the area of the river valleys researched.

4.2 Topographic slope and micro-landform

With ArcGIS software, we firstly built DEM of the studied areas by the contour line oin 1∶50000 scale and produced a slope figure, then we classified the slope figure and made a spatial statistics analysis for the geohazards and the slope grading figure, and finally we got the results as listed in Table 4 and Figure 11. Most seismogenic geohazards are distributed on the slopes from 20° to 50°, accounting for 86.8% of the total numbers. The density of geohazards on the slopes from 40° to 50° degrees is the highest. Earthquake geohazards seldom were found on the topographical slopes less than 20°. Therefore, the area of relatively gentle topographic slope is chosen as the rebuilding sites in the rebuilding work after the earthquake, where potential geohazards dangers would be quite low.

By further field investigation, we have found that there is a close relationship between the specific positions of the seismogenic geohazards and micro-landform. The seismogenic geohazards usually happen in the fol

Table 3 Relationship between distribution of geohazards and elevation

Elevation (m)	Area (km^2)	Number of geohazards	Geohazards/km^2
<650	4065.7	228	0.06
650－1000	4143.52	2239	0.54
1000－1500	5587.82	3524	0.63
1500－2000	4519.95	2471	0.55
2000－2500	3961.52	1408	0.36
>2500	30097.96	1438	0.05

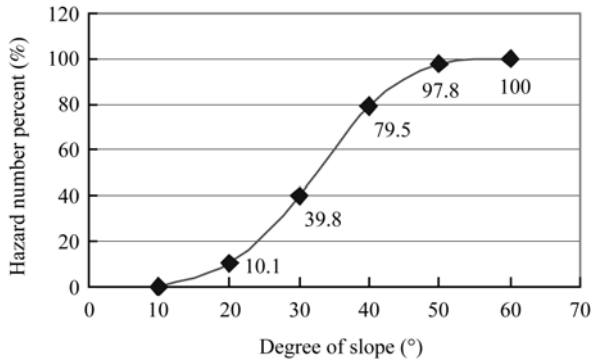

Figure 11 Correlation curve of geohazards distribution and slope.

lowing positions: (1) the transitional and turning position of gentle topographic slope to steep slope; (2) sharp edges; and (3) isolated mountain or full-space mountain position.

4.3 Lithology

The lithologic layers (including soil) in the areas studied could be classified into 8 categories: Soil, sandstone, sandy conglomerate, sand-slate, phyllite, argillite, carbonate rock and magmatic rock. The spatial statistic analysis of the geohazards and lithologic layers showed that the geohazards in hard rock layers, including magmatic rock, carbonate rock and sandy conglomerate, were the most developed, and that the development density of sand-slate, phyllite and argillites were the second. Table 5 is the relationship between distribution of geohazards and lithology. The field investigation also showed that the two types of the geohazards in rock layers were different: Collapses usually occur in hard rocks, while landslides usually occur in soft rocks.

5 Conclusions

(1) The seismogenic geohazards of Wenchuan Earthquake demonstrated the significant characteristics of zonal distribution along the coseismic fault zone and linear distribution along the rivers. The distribution of the geohazards has marked hanging wall effect, i.e., the development density of the geohazards in the hanging wall of coseismic fault zone was obviously higher than that in the foot wall. The distribution and development density of the geohazards to the northeast of epicenter was obviously stronger than that to the southwest.

(2) The nearer the area was from seismogenic faults, the higher the development density of geohazards was. The range of 10 km in the hanging wall of seismogenic faults was the strong development zone of the geohazards. The range from 10—20 km was a medium developed zone.

(3) Most collapses happened below the elevation of 1500—2000 m. This range of elevation was corresponding to the elevation range of the area through which the dale transitted to canyon, being in the position of quite steep topographic slope, rather strong rock mass unloading and the most prominent seismic response in the river bank slope.

Table 4 Relationship between distribution of geohazards and slope

Slope (°)	Area (km^2)	Number of geohazards	Geohazards/km^2
10—20	5632.67	928	0.16
20—30	14603.37	2716	0.19
30—40	13984.8	3631	0.26
40—50	5048.27	1678	0.33
>50	913.14	200	0.22

Note: Due to the positional error made when compiling the hazards acquired from field investigation into the figure, many hazards are distributed within the range of less than 10°. This does not match the actual situation, so these hazards are excluded from the statistic analysis.

Table 5 Relationship between distribution of geohazards and lithology

Lithology	Area (km^2)	Number of geohazards	Geohazards/km^2
Soil layer	3595.38	93	0.03
Sandstone	15265.49	1760	0.12
Sandy conglomerate	560.18	213	0.38
Sand-slate	11022.43	1665	0.15
Phyllite	4803.88	755	0.16
Argillutite	3599.81	631	0.18
Carbonate rock	6774.4	2577	0.38
Magmatic rock	6755.4	3614	0.53

(4) The seismogenic geohazards were mainly distributed on the slopes of 20°—50°. There was a close relationship between the specific positions and micro-landform for the geohazards usually happening in the transitional and turning position of gentle topographic slope to steep slope, thin ridge, isolated or full-face space mountains. The amplification effect in these positions was the most striking.

(5) Generally the earthquake geohazards developed in various rock layers, but their development extent in hard rock layers such as magmatic rock, carbonate rock and glutinite was greater than that in soft rock layers such as sand-slate, phyllite and argillutite. The collapses usually happened in hard rock layers, while landslides usually happened in soft rock layers.

(6) Remote-sensing interpretation by using middle & high resolution satellite images combined with high-accuracy aerial images is an effective way to quickly and fully acquire the spatial distribution of earthquake geohazards in earthquake-hit regions. It can timely provide important basic data for earthquake rescue and relief and post-earthquake reconstruction.

1 Parsons T, Ji C, Kirby E. Stress changes from the 2008 Wenchuan earthquake and increased hazard in the Sichuan basin. Nature, 2008, 454(7203): 509—510

2 Huang R Q, Xu Q. Catastrophic Landslides in China (in Chinese). Beijing: Science Press, 2008. 1—553

3 The Front Line Headquarter of Ministry of Land and Resource for Earthquake Rescue and Disaster Relief. Emergency hunting report of geohazards in the disaster area of "5·12"Wenchuan Earthquake, 2008

4 Abrahamson N A, Somerville P G. Effects of the hanging wall and footwall on ground motions recorded during the Northridge earthquake. Bull Seism Soc Amer, 1996, 86(1B): S93—S99

5 Abrahamson N A, Silva W J. Empirical response spectral attenuation relations for shallow crustal earthquakes. Seism Res Lett, 1997, 68(1): 94—109

6 Boore D M, Joyner W B, Fumal T E. Equations for estimating horizontal response spectra and peak acceleration from western North American earthquakes: a summary of recent work. Seism Res Lett, 1997, 68(1): 128—153

7 Campbell KW. Empirical near-source attenuation relationships for horizontal and vertical components of peak ground acceleration, peak ground velocity, and pseudo-absolute acceleration response spectra. S eism Res Lett, 1997, 68(1): 154—179

8 Sadigh K, Chang C Y, Egan J A, et al. Attenuation relationships for shallow crustal earthquakes based on California strong motion data. Seism Res Lett, 1997, 68(1): 180—189

9 Lin Q W, Lai W J, Huang M L, et al. The cause of the 1999 Chi-Chi earthquake in Taiwan and its fault active mechanism (in Chinese). Nat Sci Newslett, 1999, 11(4): 147—155

10 Yu Y X, Gao M T. Effects of the hanging wall and foot wall on peak acceleration during the Chi-Chi earthquake, Taiwan (in Chinese). Acta Seismologica Sinica, 2001, 23(6): 615—621

11 Chen Y T. Why was Wenchuan Earthquake so serious. http://www.sciencenet.cn/htmlnews/2008/6/200862781145413208421.html

12 Chen Y T. On the Magnitude and the Fault Length of the Great Wenchuan Earthquake (in Chinese). Sci & Tech Rev, 2008, 26(10): 26—27